

Deep Surveys of Massive Black Holes with LISA

Alberto Vecchio

*Max Planck Institut für Gravitationsphysik, Albert-Einstein-Institut
Am Mühlenberg 1, D-14476 Golm, Germany*

Abstract. Massive black hole binary systems – with mass in the range $\sim 10^5 M_\odot - 10^8 M_\odot$ – are among the most interesting sources for the Laser Interferometer Space Antenna (LISA); gravitational radiation emitted during the last year of in-spiral could be detectable with a very large ($\sim 10^3$) signal-to-noise ratio for sources at cosmological distance. Here we discuss the impact of LISA for astronomy and cosmology; we review our present understanding of the relevant issues, and highlight open problems that deserve further investigations.

INTRODUCTION

The Laser Interferometer Space Antenna (LISA) [1] is a gravitational wave (GW) observatory in the low-frequency band which is currently accessible only through non-dedicated (and low sensitivity) experiments based on the technique of Doppler tracking of interplanetary spacecraft [2,3]. As of this writing, LISA is identified as an ESA Cornerstone mission in the Horizon 2000-plus program, but is presently studied by both ESA and NASA with the view of a joint mission with launching date 2008-2010. The instrument has an optimal sensitivity in the milli-Hz frequency range, $h_{\text{rms}} \approx 3 \times 10^{-22}$ for $f \sim 1 \text{ mHz}$, covering the band $\sim 10^{-5} \text{ Hz} - 30 \text{ mHz}$. It consists of a constellation of three drag-free spacecraft placed at the vertices of an ideal equilateral triangle with sides of $\simeq 5 \times 10^6 \text{ km}$, forming a three-arms interferometer [1,4].

The low frequency band is populated by a *plethora* of GW sources, that are out of reach for Earth-based detectors, and could be easily detectable by LISA [1]: they include *guaranteed* sources, such as *known* galactic short-period binary stars; neutron stars (NS's) and/or low-to-intermediate mass black holes ($\sim 10 M_\odot - 10^3 M_\odot$) falling into a massive companion ($\sim 10^5 M_\odot - 10^8 M_\odot$); massive black hole binary systems (MBHB's), with mass in the range $\sim 10^5 M_\odot - 10^8 M_\odot$; stochastic backgrounds of primordial origin, and generated by the incoherent superposition of unresolved binary systems in the Universe.

The purpose of this contribution is to discuss the impact of LISA for astronomy. Being impossible to cover all aspects, we will concentrate on one specific class of sources: massive black hole binary systems. We will describe how LISA works as GW telescope – we are ultimately dealing with a new branch of observational astronomy – summarize our present understanding of the main issues, and highlight open questions that deserve further investigations.

MBHB's are possibly the strongest sources of GW's that LISA will be able to detect; for typical objects of mass $\sim 10^6 M_\odot$ at redshift $z \sim 1$, the signal-to-noise ratio (SNR) is $\sim 10^3$, as show in Fig.1. The instrument is able to detect the

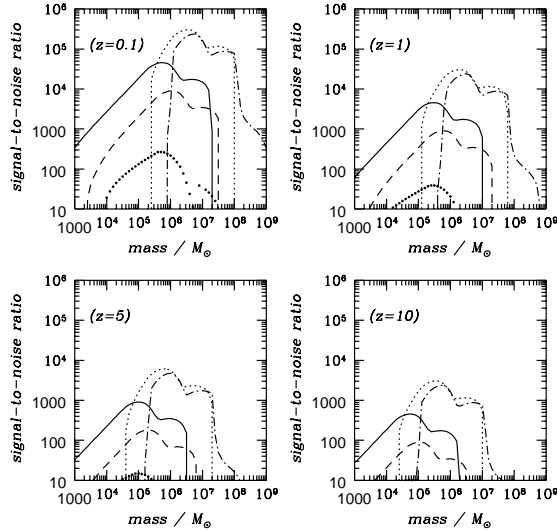


FIGURE 1. The sensitivity of LISA to coalescing black hole binary systems. The plots show the angle-averaged signal-to-noise ratio which characterizes LISA observations of the three phases of BH coalescence – in-spiral, merger, and ring-down – as a function of the mass m_1 of the primary object. The solid, dotted and dotted-dashed lines refer to the in-spiral, merger and ring-down signal, respectively, of two BH's with $m_1 = m_2$; the dashed line and the bold dots describe the in-spiral signal from two BH's with $m_1 = 100 m_2$, and a secondary BH of $10 M_\odot$ orbiting m_1 , respectively. The SNR of the in-spiral signal refers to the final year of the source life, with cut-off frequency $f_{\text{isco}} \simeq 4.4 \times 10^{-3} [m(1+z)/10^6 M_\odot]^{-1}$; the quasi-normal ringing is assumed to occur at $f_{\text{qnr}} \simeq 6.5 \times 10^{-2} [m(1+z)/10^6 M_\odot]^{-1}$, and the energy radiated during the merger and the ring-down phases are computed according to [5]. The four panels refer to different distances of the fiducial source, where we adopt, for simplicity, a luminosity distance given by $D = z/75 \text{ km sec}^{-1} \text{ Mpc}^{-1}$. The instrument low and high frequency cut-offs are (conservatively) 10^{-4} Hz and $3 \times 10^{-2} \text{ Hz}$, respectively. The noise spectral density takes into account both the instrumental noise and the so-called confusion noise [6,7].

radiation emitted during one (or more) of the three phases of black hole coalescence (in the GW jargon: in-spiral, merger, and ring-down) for a very wide range of masses – in principle from $\sim 1 M_\odot$ to $\sim 10^9 M_\odot$, depending on the mass m_1 and m_2 , and the source distance – see Fig. 1, possibly beyond redshift $z \sim 5$, if BH’s do already exist, and are involved in catastrophic events with copious release of energy through GW’s.

LISA will be able to carry out a deep and extensive census of black hole populations in the Universe, providing an accurate demography of these objects and their environment. Compelling arguments suggest the presence of MBH’s in the nuclei of most galaxies, and they are invoked to explain a number of phenomena, in particular the activity of quasars and active galactic nuclei [8,9]. However, the observational evidences of MBH existence come mainly from observations of relatively nearby galaxies, whose nuclei do not show significant activity [10–12]. Massive black holes seem to be clustered in the mass-range $10^6 M_\odot - 10^9 M_\odot$ [13]; at the lower edge of the BH mass-spectrum, we find evidences for solar-mass BH candidates [14]. No information is presently available regarding BH’s with mass between $\sim 10 M_\odot$ and $\sim 10^6 M_\odot$, although some recent X-ray observations are interpreted as possible (but not compelling) indications of "middleweight" BH’s [15,16]. LISA – and Earth-based laser interferometers – will definitely show whether this gap is simply due to a "selection" effect of present electro-magnetic observations, or indeed Nature does not provide intermediate mass black holes: an important feature of LISA is its capability of detecting BH’s with mass $\sim 10^3 M_\odot - 10^4 M_\odot$, still far from coalescence at high redshift, see Fig. 1. LISA is also likely to monitor binary systems with a wide spectrum of BH spins and orbital eccentricities, which will enable us to carry out high precision tests of general relativity [17–19], and to derive a map of the distribution of these physical parameters in astrophysical objects.

One of the most interesting observations would be the detection of GW’s *and* electro-magnetic radiation from the merger of two BH’s. We do not know as yet, whether a burst of electro-magnetic radiation is emitted during MBH collisions [21]. Determining where and when a MBH merger takes place, and possibly alerting in advance the astronomers is of paramount importance; this issue is directly linked to the identification of the source host galaxy: it would allow us to establish correlations between MBH’s and their environment, and use LISA observations to estimate the fundamental cosmological parameters [1,20].

We have not discussed so far the rate at which we expect to detect such signals. A fair statement would probably be that, essentially, we do not know it. However, we can summarize our present knowledge as follows. For MBHB systems, the event rate depends strongly on theoretical prejudices and model assumptions; the "canonical" value is $\sim 1 \text{ yr}^{-1}$, but rates as high as $\sim 10^3 \text{ yr}^{-1}$ or as low as $\sim 10^{-2} \text{ yr}^{-1}$ are consistent with theoretical models [21–24]. For low-mass black holes captured by a massive one in galactic cores, we believe to have a better understanding, and current astrophysical estimates yield a rate of a few events per year up to $z \simeq 1$ [25,26].

THE LISA TELESCOPE

We are dealing with a new generation of telescopes, both regarding the kind of radiation they observe (gravitational waves) and the frequency window in which they operate (\sim mHz). It is therefore instructive to analyze the features that enable LISA to extract accurate information about GW sources.

We consider here only the in-spiral portion of the whole coalescence waveform, neglecting the merger and ring-down, both easily detectable, cfr. Fig. 1. The merger waveform is still poorly understood from the theoretical point of view; significant progresses have been made using either full numerical schemes or semi-analytical approximations, but both approaches are still far from returning a satisfactory answer for GW observations (see [27,28] and references therein). We do however expect to gain key information by detecting GW's emitted during the final plunge, for instance how energy and angular momentum are radiated during this extreme strong-gravity phase. The ring-down signal, on the contrary, is theoretically well known; in order to limit the level of complexity of our analysis, we do not include it into the signal that we consider here; however, future investigations should keep it (as well as the final plunge, if/when available) into account, as it might change (conceivably improve) LISA performances in a number of astrophysical situations.

There are two main features that distinguish the in-spiral signals recorded by LISA from the ones that we expect to detect with Earth-based interferometers: (i) they last for months-to-centuries (depending on the masses) in the instrument observational band, and therefore are not burst-signals; in fact, the (Newtonian) time to coalescence is $\tau \simeq 1.2 \times 10^7 (f_0/10^{-4} \text{ Hz})^{-8/3} [m(1+z)/10^6 M_\odot]^{-5/3} (\eta/0.25)^{-1}$ sec; here $m = m_1 + m_2$ is the total mass, and $\eta = \mu/m$ is the symmetric mass ratio, where $\mu = m_1 m_2 / m$ is the reduced mass; (ii) the structure of the waveform is in general much more complex; in fact, we can expect to detect black holes that are fast spinning *and* live on highly elliptical orbits, in particular for the extreme mass ratio case, $\eta \ll 1$ [29]. As an example, in LIGO observations one will likely monitor no more than 10 cycles of precession of the orbital plane and the spins, whereas in the LISA band, for a typical observation time of 1 year, they could be as many as ~ 1000 , see Table 1.

An useful figure, for both detection and parameter estimation, is also the number

TABLE 1. The number of precession cycles observed by LISA. The table shows the number of cycles ($\mathcal{N}_{\text{prec}}$) of $\hat{\mathbf{L}}$ and $\hat{\mathbf{S}}$ around the constant direction of the total angular momentum $\mathbf{J} = \mathbf{L} + \mathbf{S}$ during the final year of in-spiral for BH binary systems with selected masses (in units of M_\odot) and spins.

S/m^2	m_1	m_2	$\mathcal{N}_{\text{prec}}$									
0.95	10^7	10^6	11	10^6	10^6	25	10^6	10^5	23	10^6	10^2	1262
0.50	10^7	10^6	7	10^6	10^6	20	10^6	10^5	16	10^6	10^2	708
0.10	10^7	10^6	4	10^6	10^6	16	10^6	10^5	9	10^6	10^2	150
0.01	10^7	10^6	3	10^6	10^6	16	10^6	10^5	8	10^6	10^2	16

of wave cycles recorded by LISA: during the final year of in-spiral, they range from $\sim 10^3$ (for $m_1 \sim m_2$) to $\sim 10^5$ (for $\eta \ll 1$).

In general, 17 parameters describe the waveform. No analysis has been carried out so far dealing with such general situation. Here, we will introduce some simplifying assumption, while retaining most of the key physical ingredients. The main limitation of our approach derives from considering circular orbits; this is probably quite realistic for binary systems of two MBH's which have undergone a common evolution inside a galactic core, but is almost for sure violated for solar mass compact objects and/or low mass BH's orbiting a massive one [29]. We do, however, take into account spins; in this case we assume that either the masses of the BH's are roughly equal, or one of the BH's has a negligible spin (which still describe a wide range of astrophysical situations): the binary system undergoes the so-called *simple precession* [30], where the orbital angular momentum \mathbf{L} and the total spin $\mathbf{S} = \mathbf{S}_1 + \mathbf{S}_2$ are locked together, and precess around the (almost) constant direction of the total angular momentum $\mathbf{J} = \mathbf{S} + \mathbf{L}$. We also use the post^{1.5}-Newtonian approximation of the GW phase [31]. As a consequence of this chain of approximations, the number of parameters describing the signal drastically reduces, from 17 to 11.

It is useful now to review some of the instrumental features, in order to understand how LISA works as GW observatory:

(i) LISA is an *all-sky monitor*, and one gets for free all-sky surveys. During the observation time, however, LISA changes location and orientation. The LISA orbital motion is rather peculiar – the baricenter of the instrument is inserted in a heliocentric orbit, following by 20° the Earth; the detector plane is tilted by 60° with respect to the Ecliptic and the instrument counter-rotates around the normal to the detector plane with the same 1-yr period – and is conceived in order to keep the configuration as stable as possible during the mission, as well as to give optimal coverage of the sky. It also turns out to be a key factor in reconstructing the source location in the sky.

(ii) The sources are distinguished in the data stream by the different structure and time evolution of the signals at the detector output; the recorded in-spiral signal reads:

$$h_\alpha(t) = A_{\text{gw}}(t) A_p^\alpha(t) \cos[\phi_{\text{gw}}(t) + \varphi_p^\alpha(t) + \phi_D(t)] \quad (1)$$

where $A_p(t)$ and $\varphi_p(t)$ are the time-varying polarization amplitude and phase, respectively, and $\phi_D(t)$ is the Doppler phase shift induced by the motion of the detector around the Sun; an example of in-spiral signal at the output of LISA is given in Fig. 2. The signal is therefore amplitude and phase modulated by the motion of the LISA centre-of-mass around the Sun, the change of orientation of the detector arms, and of the binary orbital plane. All these effects encode information about some of the source parameters.

(iii) There is only one LISA detector currently planned; correlations and/or time-of-flight measurements are not possible; they would be highly desirable in order to

improve the estimation of the source parameters, in particular the source location and distance; however, as the gravitational wavelength is $\lambda_{\text{gw}} \simeq 2 (f/1 \text{ mHz})^{-1} \text{ AU}$, a second detector would have to be placed at several AU from the first one in order to provide useful information on the position of a source in the sky; however LISA is a three-arms instrument; Cutler [32] has shown that the outputs from each arm can be combined in such a way to form a pair of data sets, $\alpha = 1, 2$ in Eq. (1), whose noise is uncorrelated at all frequencies, that are equivalent to the data streams recorded by two co-located interferometers, rotated by $\pi/4$ one with respect to the other.

Indeed, there will be two data streams available to extract all source parameters. Correlations between the parameters are inevitable, and conspire to degrade the accuracy of the parameter measurements. It should also be clear that for LISA the measurement errors depend crucially on the actual value of the source parameters, and one therefore needs to explore a very large parameter space to give a fair description of the instrument performances.

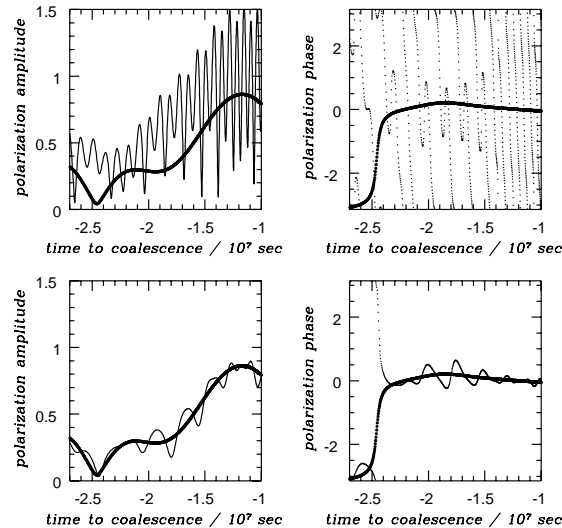


FIGURE 2. In-spiral signals at the LISA output. The plots show the evolution of the polarization amplitude $A_p(t)$ (on the left) and phase $\varphi_p(t)$ (on the right) as a function of time, cfr. Eq. 1, for black holes with $S = 0$ (bold solid line) and $S \neq 0$ (thin solid line, for $A_p(t)$, and dotted line, for $\varphi_p(t)$). The two plots at the top refer to a source with masses $m_1 = 10^7 M_\odot$ and $m_2 = 10^5 M_\odot$; in the case of spinning black holes the parameters are: $S/m^2 = 0.95$, $\hat{\mathbf{S}} \cdot \hat{\mathbf{L}} = 0.5$. The plots at the bottom refer to a MBHB with $m_1 = m_2 = 10^6 M_\odot$: when spins are present the choice of parameters is according to: $S/m^2 = 0.3$, and $\hat{\mathbf{S}} \cdot \hat{\mathbf{L}} = 0.9$.

SURVEYS OF MASSIVE BACK HOLES

We have discussed in the Introduction the sensitivity of LISA: there is little doubt that such interferometer will be able to survey a fairly large fraction BH populations in the Universe. We would like to stress that in the present discussion, we assume to be able to monitor the whole final year of in-spiral. This is a key and delicate point which affects the capability of surveying sources at increasingly higher z and/or with larger m , and measuring precisely the parameters: in fact, at some frequency (between 10^{-4} Hz and 10^{-5} Hz) the instrumental noise will completely dominate the signal, allowing to pick up only the very final portion of the in-spiral (say a few days), or even preventing the detection; the redshifted radiation simply falls outside the observational band, cfr. Fig. 1. It is clear that the higher the redshift, the lower the typical mass for which LISA reaches the optimal sensitivity. Super-massive black holes of mass $\sim 10^9 M_\odot$ might be observable, by detecting ring-down

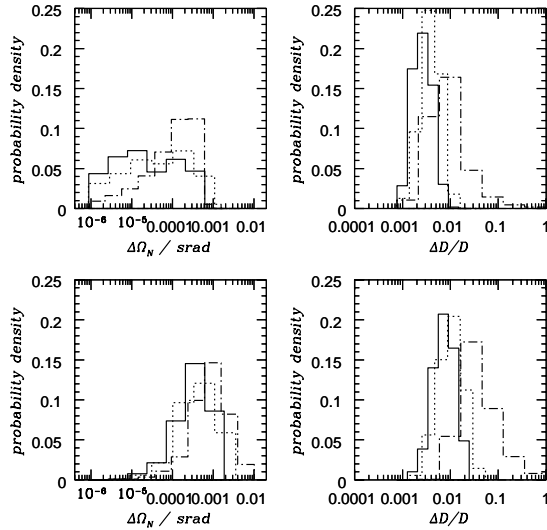


FIGURE 3. The probability distribution of the angular resolution $\Delta\Omega_N$ and the relative error of the distance determination $\Delta D/D$, with which LISA can identify a MBHB by observing the final year of in-spiral. The histograms show the result of a Monte-Carlo simulation, where 1000 sources, with masses $m_1 = m_2 = 10^6 M_\odot$ at redshift $z = 1$, have been randomly located and oriented in the sky. The top panels refer to measurements carried out by both LISA detectors, whereas the bottom panels report the results obtained by using only a single interferometer. The plots compare the estimated errors in the measurement of the parameters assuming three different values of the spin: $S/m^2 = 0.9$ (solid line), 0.3 (dotted line), and 0 (dotted-dashed line). The total noise is given by the sum of the instrumental noise and the confusion noise.

signals at low redshifts ($z \lesssim 0.1$), if the sensitivity window extends to $\sim 10^{-5}$ Hz.

Several analysis have been carried out so far dealing with the accuracy of the parameter measurements with LISA [32–36]; however, they have been mainly focussed on investigations of the instrument angular resolution; moreover, spin effects have been either ignored or explored for a very limited portion of the total parameter range. Here we will try to give a more comprehensive description of the performances of LISA as GW observatory. The accuracy of the parameter measurements is very sensitive to the actual source parameter values; it is therefore almost impossible to give *typical figures* for LISA as GW telescope, that can be applied to a wide range of binary systems. We discuss in some detail the case of an equal-mass MBHB, with $m_1 = m_2 = 10^6 M_\odot$, and give some general criteria to extend these results to other parameter values. It turns out that the source location and orientation with respect to the detector play a key role. We have therefore performed Monte-Carlo simulations, where we fix the source distance and the physical parameters, and vary randomly the "geometrical" parameters, $\hat{\mathbf{N}}$, $\hat{\mathbf{J}}$ and $\hat{\mathbf{S}}$. We compute the estimated mean squared errors associated to the parameter measurements by means of the so-called *variance-covariance* matrix [37,38].

The main results are presented in Figs. 3 and 4, and can be summarized as follows. The angular resolution is $\Delta\Omega_N \sim 10^{-5}$ srad; however, depending on

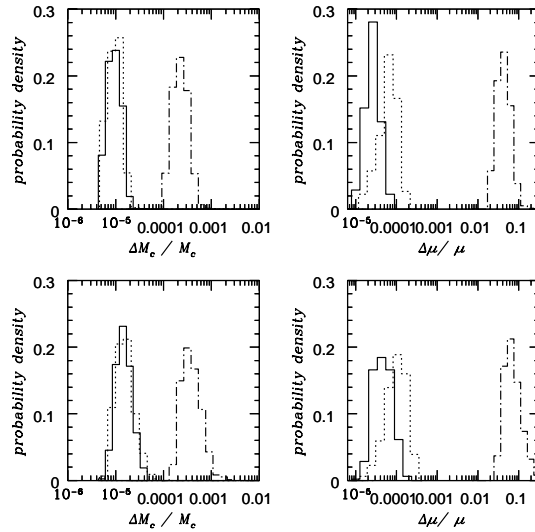


FIGURE 4. The probability distribution of the errors with which the source masses can be measured by LISA in one year of observation. Same as Fig. 3, but now the histograms show the distribution of the errors regarding the mass parameters, where our choice corresponds to the chirp mass, $\Delta M_c/M_c$ (panels on the left), and the reduced mass, $\Delta\mu/\mu$ (panels on the right).

the location and orientation of the source it varies over a wide range of values, $10 \text{ arcmin}^2 \lesssim \Delta\Omega_N \lesssim 3 \text{ deg}^2$. Typically, large spins and misalignment angles – the angle between $\hat{\mathbf{L}}$ and $\hat{\mathbf{S}}$ – allow us to measure more precisely the source location; for a small region of these parameters, the "error-box" in the sky could possibly be only a fraction of arcmin^2 . The distance is usually measured with an error $0.1\% \lesssim \Delta D/D \lesssim 1\%$. The timing accuracy is very high, and the instance of coalescence can be identified within ~ 10 sec. Masses and spins can be measured very precisely; typically, the errors affecting the determination of the chirp and reduced mass are $\Delta\mathcal{M}/\mathcal{M} \sim 10^{-5}$ and $\Delta\mu/\mu \sim 10^{-4}$, respectively; the so-called spin-orbit parameter β can be determined with an error $\Delta\beta \sim 10^{-3}$. There is one general rule that can be derived from this analysis: if BH's are highly spinning and the misalignment angle is large, the parameter determination improves. This is due to the fact that the parameters leave peculiar finger prints on the recorded signal, cfr. Fig. 2: in particular, A_p and φ_p undergo strong modulations, which carry information not only on the position of the source and the orientation of the angular momenta, but also on the physical parameters, such as the masses. This is an effect which is similar – although the physics behind it is different – to the one that takes place when spins are not present, but one considers not only radiation emitted at twice the orbital frequency, but also at other harmonics [35] (notice that in Fig. 3 and 4, for the case $S = 0$, we report results obtained considering only the dominant harmonic; we refer the reader to [35] for more details).

We can now ask how these results change by selecting different source parameters. MBHB's with $m_1 \sim m_2 \sim 10^7 M_\odot$ would be typically observed with larger errors, by a factor ≈ 10 , than the ones reported here. If we fix m_1 and vary m_2 , the measurement accuracy is fairly constant – within, say, a factor ≈ 2 – as long as $m_2/m_1 \gtrsim 0.1$, then it starts degrading: this is due to a rather complex competition between several effects, in particular the SNR and the number of wave/precession cycles [39,40].

MBHB's will be visible several months before the final coalescence. This will allow us to pick up the signal when the binary system is still far from merging, and refine the source parameter measurements as the source proceeds toward the deadly plunge [39]: for a limited region of the parameter space, it could be possible to determine the source location in the sky with enough precision to have a realistic chance of observing the same field with other telescopes.

REFERENCES

1. P. Bender et al., *LISA Pre-Phase A Report; Second Edition*, MPQ 233 (1998).
2. F. B. Estabrook and H. R. Wahlquist, Gen. Rel. Grav. **6**, 439 (1975).
3. B. Bertotti, A. Vecchio, and L. Iess, Phys. Rev. D **59**, 082001 (1999).
4. K. Danzmann, theses proceedings.
5. E. Flanagan and S. Hughes, Phys. Rev. D **57**, 4535 (1998).
6. D. Hils, P. L. Bender, and R.F. Webbink, Astrophys. J. **360**, 75 (1990);

7. P. L. Bender and D. Hils, *Class. and Quantum Grav.* **14**, 1439 (1997).
8. Y. B. Zel'dovich and I. D. Novikov, *Sov. Phys. Dokl.* **158**, 811 (1964).
9. E. E. Salpeter, *Astrophys. J.* **204**, L1 (1964).
10. M. Miyoshi, J. Moran, J. Herrnstein, L. Greenhill, N. Nakai, P. Diamond and M. Inoue, *Nature* **373**, 127 (1995).
11. A. Eckart and R. Genzel, *Nature* **383**, 415 (1996).
12. E. Maoz, *Astrophys. J.* **494**, L181 (1998).
13. D. Richstone et al., *Nature* **395**, A14 (1998).
14. M. J. Rees, in *Black holes and relativistic stars*, edited by R. Wald (University of Chicago Press, Chicago, 1998), pp. 79-101;
15. E. J. M. Colbert and R. F. Mushotzky, pre-print astro-ph/9901023
16. A. Ptak and R. Griffith, astro-ph/9903372
17. S. Hughes, these proceedings.
18. E. Poisson, *Phys. Rev. D* **54**, 5939 (1996).
19. F. D. Ryan, *Phys. Rev. D* **56**, 1845 (1997).
20. B.F. Schutz, *Nature* **232**, 675 (1986).
21. M.C. Begelman, R. D. Blandford, and M. J. Rees, *Nature* **287**, 307 (1980).
22. O. Blaes, these proceedings.
23. M.G. Haehnelt, *Mont. Not. Roy. Astron. Soc.* **269**, 199 (1994);
24. A. Vecchio, *Class. and Quantum Grav.* **14**, 1431 (1997).
25. S. Sigurdsson and M. J. Rees, *Mont. Not. Royal Astron. Soc.* **284**, 318 (1996).
26. S. Sigurdsson, *Class. and Quantum Grav.* **14**, 1425 (1997);
27. See the Binary Black Hole Grand Challenge Alliance web site for recent results and publications: <http://jean-luc.ncsa.uiuc.edu/>
28. J. Pullin, in *Gravitation and Relativity: At the turn of the Millennium*, eds. N. Dadhich and J. Narlikar (IUCAA, India), pp. 87-106 (1998).
29. D. Hils and P. L. Bender, *Astrophys. J.* **447**, L7 (1995).
30. Apostolatos, T. A., Cutler, C., Sussman, G. S., and Thorne, K. S., *Phys. Rev. D* **49**, 6274 (1994).
31. L. Blanchet, T. Damour, B.R. Iyer, C.M. Will and A.G. Wiseman, *Phys. Rev. Lett.* **74**, 3515 (1995).
32. C. Cutler, *Phys. Rev. D* **57**, 7089 (1998).
33. A. Vecchio and C. Cutler, in *Laser Interferometer Space Antenna*, ed. W. M. Falkner (AIP Conference Proceedings 456; 1998), pp. 101-109.
34. A. Vecchio, in *Recent Development in General Relativity*, ed. F. Francaviglia, (Springer Verlag), pp. 221-238), 1999.
35. A. Sintes and A. Vecchio, these proceedings.
36. T. A. Moore and R. W. Hellings, gr-qc/9910116.
37. C. Cutler and E. E. Flanagan, *Phys. Rev. D* **49**, 2658 (1994).
38. D. Nicholson, and A. Vecchio, *Phys. Rev. D* **57**, 4588, (1998).
39. A. Vecchio, C. Cutler and A. Sintes, in preparation.
40. A. Vecchio, in preparation.